Scanning Microscopy

Volume 1992
Number 6 *Signal and Image Processing in Microscopy and Microanalysis*

Article 34

1992

Cathodoluminescence Image Processing of High TC Superconductors

Z. Barkay
Tel Aviv University, Israel

G. Deutscher
Tel Aviv University, Israel

E. Grunbaum
Tel Aviv University, Israel

Scanning Microscopy Supplement 6, 1992 (pages 369-378) 0892-953X/92$5.00+.00
Scanning Microscopy International, Chicago (AMF O'Hare), IL 60666 USA

CATHODOLUMINESCENCE IMAGE PROCESSING OF HIGH T_C SUPERCONDUCTORS

Z. Barkay*, G. Deutscher, E. Grunbaum+

School of Physics and Astronomy, Raymond and Beverly Sackler Faculty of Exact Sciences, and
+Department of Physical Electronics, Faculty of Engineering
Tel Aviv University, 69978 Ramat Aviv, Israel

Abstract

Cathodoluminescence (CL) in the Scanning Electron Microscope (SEM) was performed for both ceramic pellets and thin films of YBaCuO high T_C superconductors. Image processing provided additional quantitative information. For single phase films, we demonstrated the possibility to create thickness maps in real time from the CL pictures. The gradual thickness variation within the sample was revealed by the histogram of the thickness image. The continuity of the film was observed at a few threshold thicknesses values, defined by the fraction of the occupied area. At the conduction threshold value, the location and width of the conducting paths could be estimated. The analysis was of a lateral resolution better than 1 μm and of a submicron thickness resolution. Insulating impurity grains embedded in the YBaCuO ceramic pellet, which could not be recognized by secondary electrons, were revealed by the CL mode in the SEM. Their long luminescence lifetime was recorded at different time scales and provided an estimation of the lifetime and density of generated carriers. This analysis can be applied to any other high T_C superconductors.

Key Words: Cathodoluminescence, image-processing, scanning electron microscopy, high-T_C superconductors, YBaCuO, thin film, carrier life-time.

*Address for correspondence:
Z. Barkay
School of Physics and Astronomy
Tel-Aviv University
69978 Ramat Aviv, Tel-Aviv, Israel
Telephone No.: (972)-3-6408286
FAX No.: (972)-3-6422979

Introduction

The investigation of high T_C superconducting samples in the Scanning Electron Microscope (SEM) provides detection of inhomogeneities at a high spatial resolution. The principle of cathodoluminescence (CL) is the recombination of pairs of electrons-holes, which are produced by the primary electron beam, via the luminescence centers. The cathodoluminescence is thus sensitive to the electronic structure of the samples i.e., to the existence of a band gap near the Fermi energy and to localized states. Therefore, the CL in SEM has been used to differentiate between the high T_C superconducting phase and its related semiconducting and insulating phases. Both cathodoluminescence[11] and Thermally Stimulated Luminescence[3] (TSL) measurements of ceramic pellets have shown that the insulating phases, of the YBaCuO related compounds, are much more luminescent than the YBaCuO superconducting phase itself. The observed TSL from YBaCuO superconducting pellets was claimed[4] to be due to the poor oxidation surface of the material.

In the YBaCuO thin films there may be other forms of inhomogeneities in addition to the impurity phases. The variety of techniques for preparing the high T_C superconductors, such as Metal Organic Chemical Vapor Deposition (MOCVD), laser ablation or boat evaporation, results in different morphologies and thickness inhomogeneities. Many superconducting properties depend on the film thickness, the most obvious of which is the critical current density. The ability to observe thickness variations in these materials is of a great importance.

In previous[1] work we reported a CL study of high T_C superconducting thin films in the SEM. It was shown that for thin films the contribution of the substrate luminescence should be taken into account at a high primary beam energy. Thickness variations of a single high T_C superconducting phase could be observed by the decay in the substrate luminescence signal through the film. Variations in the CL intensity might also arise due to substrate imperfections, such as scratches and bright island-like defects. These irregularities were shown to have distinct geometries which could be distinguished from thickness variations.

In the present work we used a more quantitative approach by performing image processing combined with the CL measurements in SEM. It served to study two main

aspects of YBaCuO high T_C superconductors: a) thickness variation within a single phase film, to which the larger part of this paper will be devoted, and b) the long luminescence lifetimes of impurity phases in pellets. For thin films, in regions free of defects, the CL images were transformed in real time to thickness maps. This provided local information about the sample continuity and morphology. The lateral and thickness resolution of the method will be discussed as well. For ceramic pellets, the derived lifetime of the luminescence signal was used to estimate the density of carriers generated by a stationary electron beam in the insulating region.

Experimental Details

Our experiment consisted of two stages. In the first stage CL pictures were produced in the SEM, usually at long recording times. These pictures were then analyzed in the image processing system.

The CL system in the SEM had two pairs of Philips CL detectors. The CL detector was composed of a focusing lens, optical waveguide, and a photomultiplier for the spectral range of 290-675 nm. We varied the beam energy in the whole available range up to 30 keV and observed the CL intensity, as was demonstrated in our previous[1] work. The maximum CL intensity was obtained for 30 keV in the thin films. The SEM standard conditions were therefore: beam energy of about 30 keV, spot size of 200 nm, and beam current of 10^{-9} A. The present samples were studied at room temperature.

The CL pictures were taken at slow scan for the following reasons: (a) the low luminescence of the YBaCuO material required a long integration time to improve the signal to noise ratio, and (b) both the insulating impurity phases in the YBaCuO and the substrates for the thin films possess a long luminescence lifetime, which causes smearing of the initial signal at a quick scan. Therefore the luminescence signal required a long recording time before digitization. The preferred conditions were 128 msec per line and 1000 lines per frame.

The image processing unit included a Charged Coupled Device (CCD) video camera with lens attachment. The camera video output was connected to an image grabber card in the IBM PC. The image was stored in the frame memory and then displayed back on a video external monitor. Look Up Tables (LUTs) were used to transform pixel intensities prior to display. Each LUT can have a different transform such as binary thresholding or contour imaging. The digitizer was operated with 512 X 512 pixels and 256 intensity levels which corresponded to the gray scale levels of the video image. According to the size of the pictures (100 - 300 μm), each pixel represented a spot of about 0.5 μm in the sample. The number of pixels was sufficient, as the corresponding spot size in the sample was comparable to the CL resolution available according to our working conditions (see results - the part on CL spatial resolution).

YBaCuO high T_C superconductors and their related compounds were examined. The samples were in form of thin films and ceramic pellets. We will refer to an YBaCuO thin film prepared by the MOCVD method on a MgO substrate. Another thin film, of BaF_2 grains on sapphire substrate, was used for resolution estimation. The YBaCuO high T_C superconducting ceramic pellets were produced in an ordinary procedure by sintering suitable quantities of Y_2O_3 , $BaCO_3$, CuO at 950 K followed by oxygen treatment at 500 K. One of such samples, which had insulating impurities embedded in it, will be presented. Pellets of the insulating initial components, such as BaF_2 and Y_2O_3 , were also produced for comparison purposes.

Table 1

Intensity(a.u)	Thickness(μm) ($\alpha=10^5 cm^{-1}$)	Relative thickness(%)
255	0	0
79	0.12 $\pm$ 0.01	52
57	0.15 $\pm$ 0.02	65
25	0.23 $\pm$ 0.04	100

Thickness Variation Within a Superconducting Film

In order to demonstrate our thickness measurement method, we refer to the previously described YBaCuO superconducting thin film, which had a particularly contrasting CL image. The inhomogeneous film is shown at figs. 1a and 1b in the CL and the Secondary Electron (SE) modes respectively, at a scale close to that of the grain size. The analysis of the CL picture was performed in point, line and region modes.

Point and line analysis

Point analysis showed the CL intensity at each point in the picture. With the assumption of homogeneous absorption of the substrate luminescence through the film, the thickness at each point is obtained by:

$$X_i = [\ \ln(I_0/I_i)\ ]/\alpha \qquad (1)$$

where α is the film absorption constant, I_0 is the substrate luminescence, and I_i is the intensity detected through thickness X_i.

Assuming that the picture was adjusted such that zero thickness corresponds to the maximum intensity (for $I_0 = 255$, $X_i = 0$), and α is estimated as $10^5 cm^{-1}$ for the opaque high T_C material, then the thickness at each point becomes: $X_i = [\ \ln(255/I_i)\ ]/10$ in units of μm. According to this method, the maximum possible measured thickness in these high T_C superconducting films is 0.55 μm (for the minimum discrete intensity of $I_i = 1$). The thickness resolution is given by: $\Delta X_i = \Delta I/(10\ I_i)$ in μm units, or:

$$\Delta X_i = (\Delta I/2550)\ \exp(10\ X_i) \qquad (2)$$

where ΔI is the intensity resolution.

If the SEM video output is directly connected to the digitizer, the whole digitizer intensity range of 256 levels will be available and the intensity resolution is one level: $\Delta I = 1$. For a typical picture of about 20 gray scale levels, as in our case, $\Delta I = 10$ and the thickness resolution is reduced by an order of magnitude. For thicknesses of $X < 1000$Å the resolution is better than 100Å, for $0.1\mu m < X < 0.32\mu m$ the

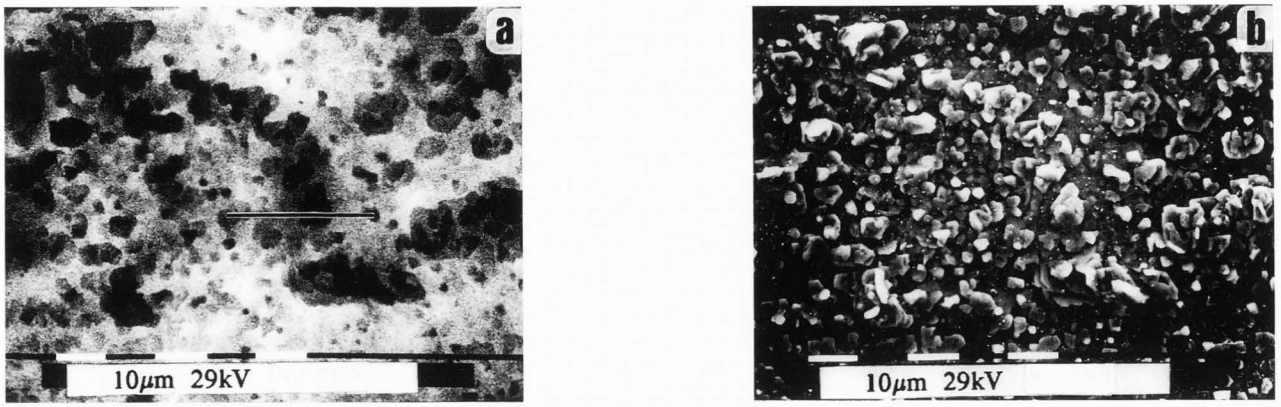

Figure 1. YBaCuO thin film: **(a)** CL micrograph, **(b)** corresponding SE micrograph.

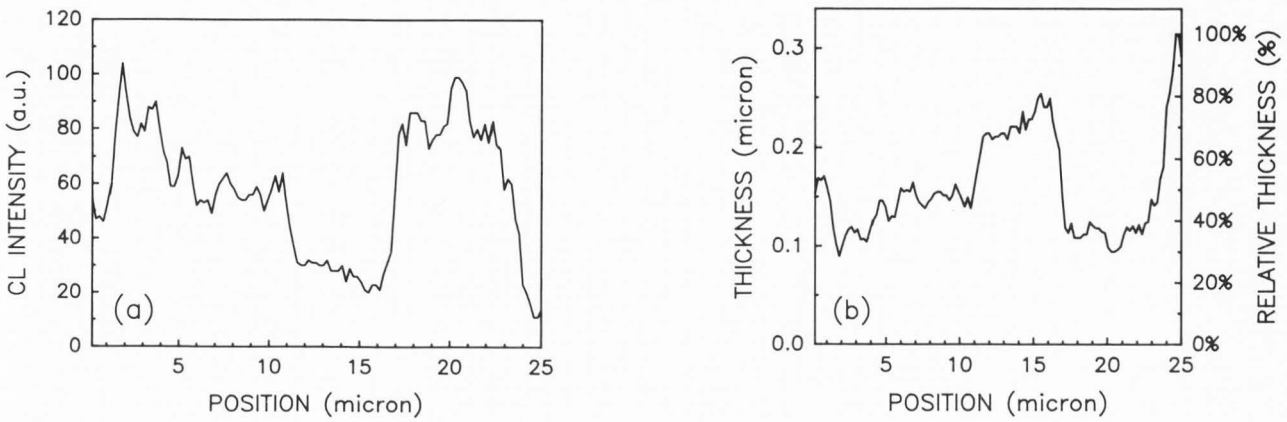

Figure 2. Line profiles along a chosen line in Figure 1a: **(a)** CL profile, **(b)** profile of the thickness and the thickness relative to the maximum value (expressed in percentage).

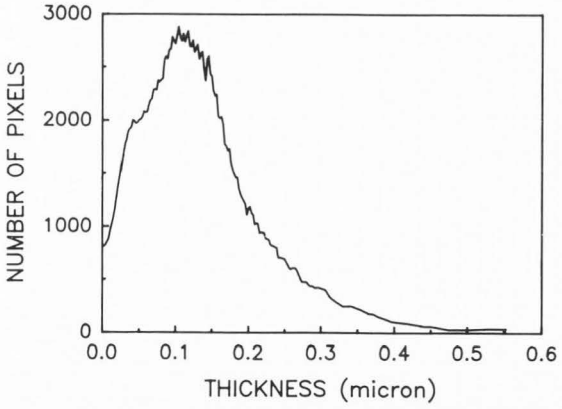

Figure 3. Histogram of the CL micrograph of Fig. 1a.

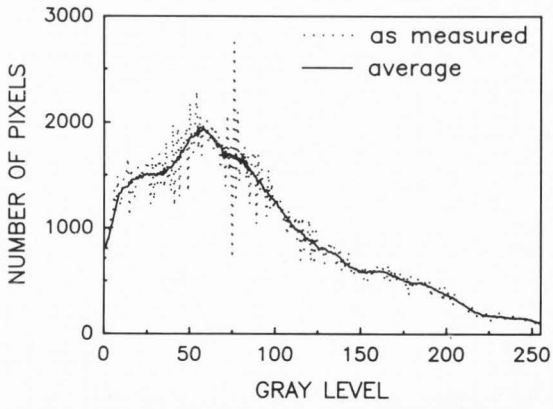

Figure 4. Histogram of the thickness image.

resolution is of order of $0.01\mu m$, and becomes of order of $0.1\mu m$ at thicknesses above $0.33\mu m$.

Table 1 shows the possibility to estimate thicknesses of random chosen points in the CL image. Four intensity values and their corresponding thicknesses (with calculated errors) are at columns 1 and 2. The values, relative to the point of maximum thickness do not depend on α (expressed in percentage in column 3).

The same procedure which was carried out for a few points was repeated for successive number of points. Graph 2a represents the CL intensity profile along a line which was chosen in fig. 1a (the line appears on the picture). Graph 2b represents the corresponding thickness values along the same line according to eq. 1. We also show the relative thickness values to that of the maximum value of the line (expressed in percentage).

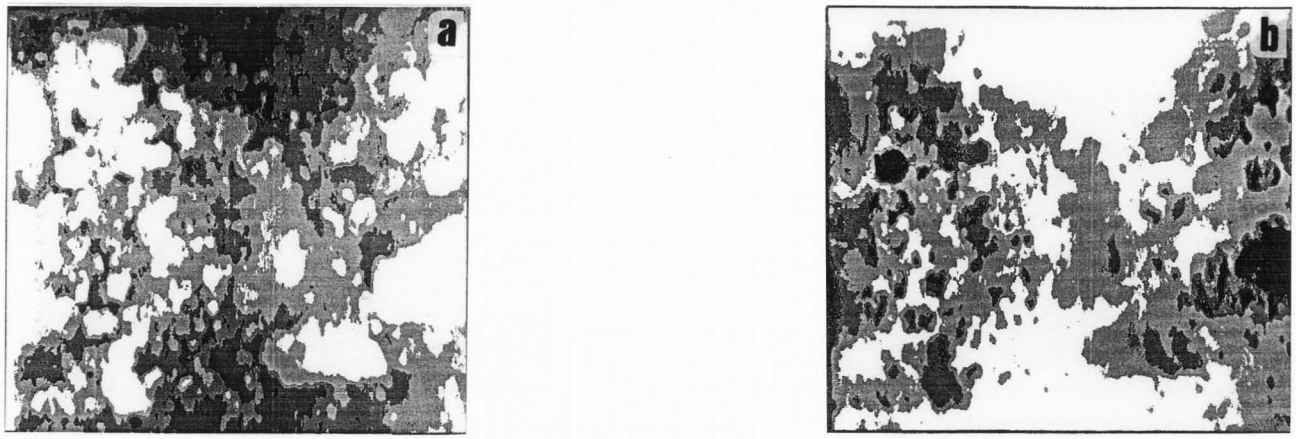

Figure 5. Computer images using five linear gray scale levels: (**a**) CL image, (**b**) thickness image.

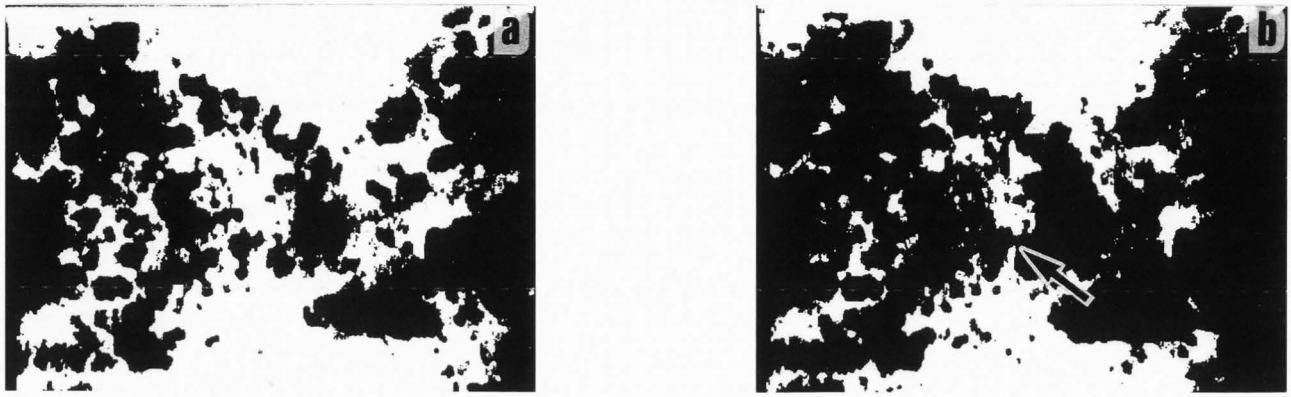

Figure 6. Computer threshold images: (**a**) 50% of occupied area, (**b**) 66% of occupied area.

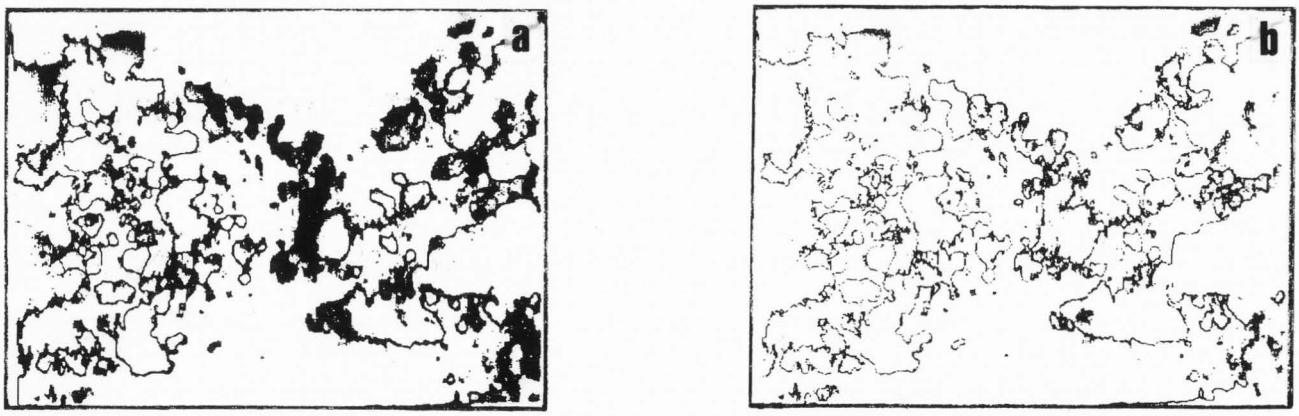

Figure 7. Computer contour images corresponding to the following peak widths : (**a**) 0.13-0.18 μm, (**b**) 0.13-0.14 μm.

Region analysis

The CL intensity image of fig. 1a could be transformed to a thickness image, when a normalized logarithmic transform, such as written in eq.1, is individually applied to each pixel in the stored image. Instead, the Look Up Table (LUT) was programmed with appropriate values to obtain the transformation in real time. The histogram of the CL image has a gradual variation over the whole gray scale range. It is shown in fig. 3 before and after smoothing over ten gray scale levels. The corresponding histogram of the thickness image (fig. 4) shows a gradual change over the thickness range. Figs. 5a and 5b represent the computer processed images of both the CL and the thickness images, using five gray scale levels of a linear intensity ratio. The

dark regions in the CL computer image correspond to the high CL intensities (or low thicknesses), and appear bright in the thickness computer image.

The histograms of figs. 3 and 4 are not bimodal gray level histograms. Therefore the threshold can not be well defined in the minimum region between the black and the white main peaks. As a criterion for defining a threshold we rather choose the fraction of the occupied area. The fraction of the occupied area is invariant under any possible shift or compression of the histograms over the gray scale or the thickness values. Fig. 6a shows the film with a threshold corresponding to 50% coverage. It appears not continuous and therefore in contradiction with a 2D random percolation model. By a gradual increase of the threshold thickness value, the fraction of the occupied area increases. For 66% of occupied area (fig. 6b), conducting paths exist and the weak links can be recognized and located (see arrow).

In addition to single threshold image maps, contour images are produced with desired upper and lower threshold boundaries defined in the CL histogram. The contour images at figs. 7a and 7b respectively correspond to intensity values of 40-70 and 60-70, which could be translated to widths of 0.13-0.18 μm and 0.13-0.14 μm. The intensities of 40-70 correspond to the maximum in the CL histogram, while the restricted range (of 60-70) exhibits only part of the peak. This approach provided mapping of specific thicknesses.

CL spatial resolution (BaF_2 sample)

The CL spatial resolution, according to our working conditions, was estimated by using an insulating thin film of well defined BaF_2 grains. Both the SE and the CL images, of the luminescent BaF_2 grain structure, were digitized. Their corresponding line intensity profiles across five grains are shown at fig. 8. The troughs in the CL signal follow the troughs in the SE signal, so that the SE resolution was maintained in the CL profile. The length of the line profile was 14.6 μm and the width of the trough in the CL profile was less than 1 μm, which is an upper limit for the scale that can be resolved.

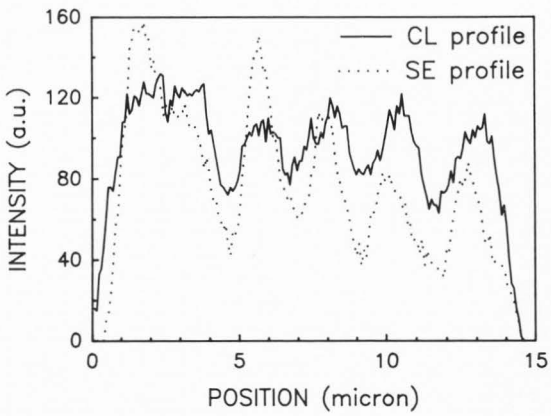

Figure 8. SE and CL line profiles along a BaF_2 thin grain film.

Luminescence Lifetime of Impurities in Superconducting Ceramic Pellets

Single phase pellets of the initial components, such as BaF_2 , Y_2O_3 or untreated mixture of the three initial YBaCuO components (with suitable ratio), charge up under the high energy beam voltage. Moreover, in previous work[2], which investigated electrical charging of percolating samples, it was found that small In grains, which are electrically isolated from a conducting In sample, charge up in the SEM. The electrical charging in the SEM usually intensifies the SE picture, and thus the nonconducting phases can be distinguished from the conducting phases. However, the SE mode was insufficient for revealing small impurities in the superconducting pellet. The high T_C bulk superconductors are of low resistance (mΩ at room temperature), and therefore small insulating impurities which are embedded in the bulk material discharge rapidly, and the SE emission appears homogeneous. By using the CL mode in SEM the impurities were well recognized.

We will refer to one of the YBaCuO pellets, of a typical grain size of a few microns, which had luminescent impurity phases (grains) embedded in it. The SE image of the pellet is seen fig. 9a. The corresponding CL pictures were taken at the following microscope time scans : 2, 8 and 32 msec per line (figs. 9b-9d). The long streaks (fig. 9b) and the shorter ones at longer time-scans (figs. 9c-9d), correspond to the luminescence signal which is collected at the CL detector after the departure of the scanning beam from the location of the luminescent grain. The grain, indicated by an arrow in fig. 9b, is observed at a higher magnification in fig. 9e, where the left size is the SE mode and the right side the CL mode. Figs. 9b-9d were digitized and then horizontal line profiles were taken across the middle of the marked grain. The profiles in fig. 10a, as well as in figs. 10b and 11a, were obtained after smoothing over a length of 7 μm along the corresponding line. In order to compare the different profiles, the 2 msec line was scaled to fit the 8 msec line (fig. 10b). The slight differences reflect the dependence of the signal to noise ratio on the time-scan.

The intense CL signal of the impurities was superimposed on the background signal of the high T_C superconductor. Therefore, the background of the CL pictures had to be obtained. Horizontal line profiles were taken across the digitized pictures in regions outside the main luminescent regions (see for example the 2 msec signal and background lines in fig. 11a). The background signal could be due to the poor oxygenation of the surface layer of the YBaCuO pellet. The variations in the background profiles fitted the variations in the SE picture, and therefore manifested the granularity and porosity of the pellet. Additional smoothing of the background line profile over a longer length scale of about 55 μm, resulted in smoothing over the topography of the specific line. Therefore, the resulting signal should be regarded as a representative background of any line across the YBaCuO region. Subtraction of this background from the original luminescence signal was shown in fig. 11b. The luminescence lifetime is estimated as the time it takes the intensity to decrease to half of its initial value. The decrease of the signal to half of its initial value is over a distance of about 100 μm (from fig. 11b), which is a part of the whole picture length of 288 μm (see fig. 9b). Considering the

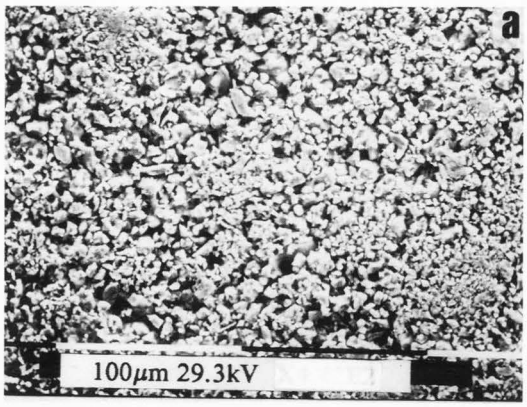

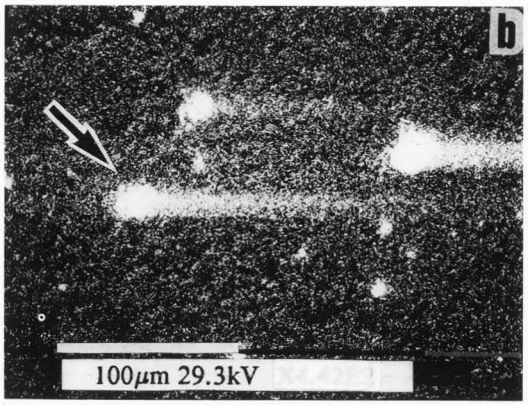

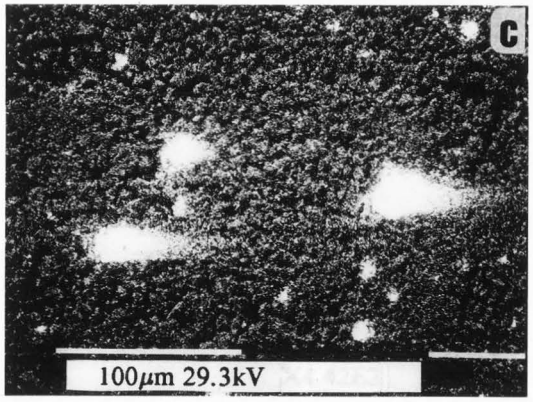

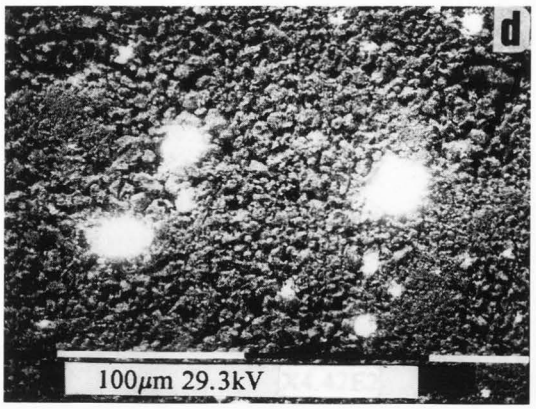

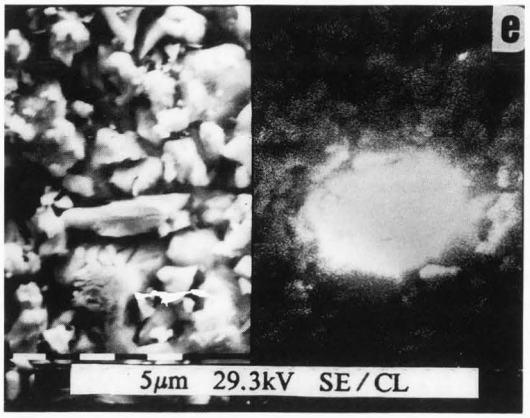

Figure 9. YBaCuO ceramic pellet: **(a)** SE micrograph, **(b)**-**(d)** CL micrographs with scan times of 2, 8 and 32 msec per line, **(e)** the grain, indicated by an arrow in Fig. 9b, at a higher magnification.

time-scan of 2 msec for the whole length, a lifetime of about 0.7 msec is obtained.

The electron-hole recombination occurs inside the volume of the impurity phase, if we neglect the diffusion of the carriers from the impurity phase into the YBaCuO superconducting phase. For a fixed beam current, it was shown[13] that the steady state density of generated carriers (Δn) in a semiconducting or insulating material is given by:

$$\Delta n \sim \frac{I_p G}{e} \frac{6}{\pi R_p^3} \tau \qquad (3)$$

when I_p is a fixed beam current, G is the gain, e stands for the electronic charge, R_p the beam penetration depth, and τ the lifetime of the generated carriers.

G is approximately obtained by the ratio $(1-\eta) \cdot E/E_i$, where η is the backscattered electron coefficient, E is the beam energy and E_i the insulator ionization energy. η is estimated for $Y_1Ba_2Cu_3O_7$ according to the Castaing expression[6] for a multicomponent target, which is $\eta = \Sigma c_i \eta_i$, where c_i is the mass fraction and η_i the coefficient of the pure element. We thus obtain $\eta = 0.33$.

The ionization energy E_i depends on the band gap (E_g) of the ceramics according to the expression[5] : $E_i \simeq 2.1\, E_g + 1.3$ [eV]. The values of band gaps of different ceramics lies in the range[14]: 3-9eV. As the emission of the luminescent grain is in the visible, E_g is at least 3eV, and therefore E_i is at least 8eV. An upper limit for E_i may be about 20eV for E_g=9eV.

R_p was shown[7] to be 2.3 μm for a 30 keV energy beam incident on YBaCuO. The luminescence lifetime may be substituted for τ, if we neglect non-radiative recombination. We substitute : $I_p = 10^{-9}$ A, E = 30 keV, $E_i \simeq$ 8eV, R_p = 2.3 μm and τ = 0.7 msec in eq.3. The maximum value for the density of carriers (Δn), which is produced in the insulator grain by a stationary current electron beam, is about $2 \cdot 10^{21}$ cm^{-3}. This value is obtained

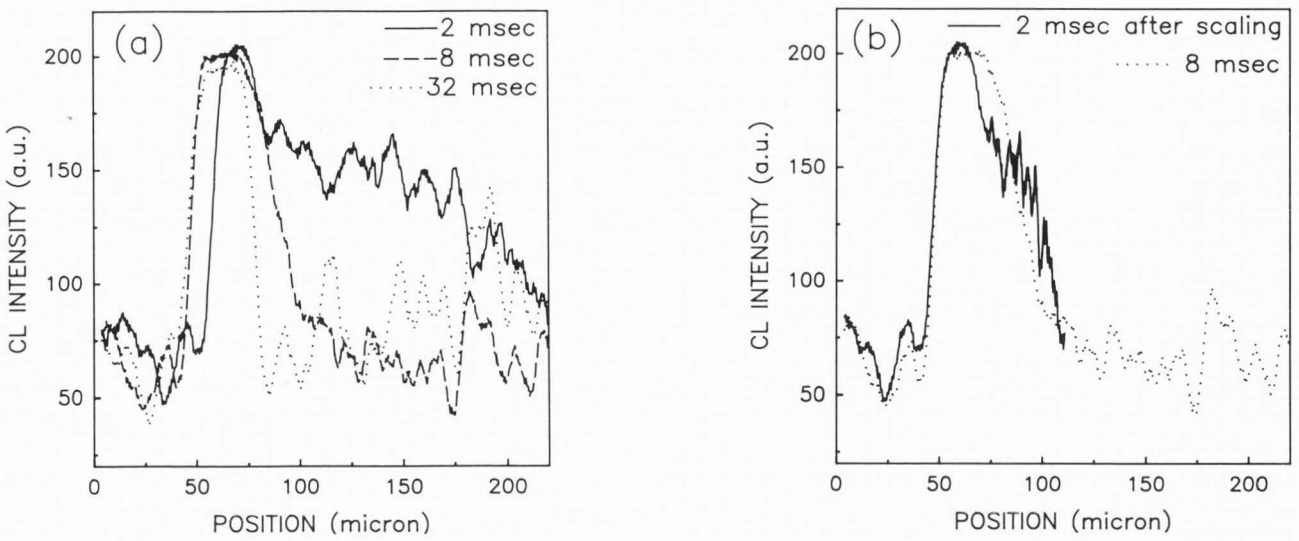

Figure 10. **(a)** Three CL line profiles corresponding to Figs. 9(b)-9(d) along the marked grain. **(b)** 2 msec CL line profile after scaling and the original 8 msec line profile.

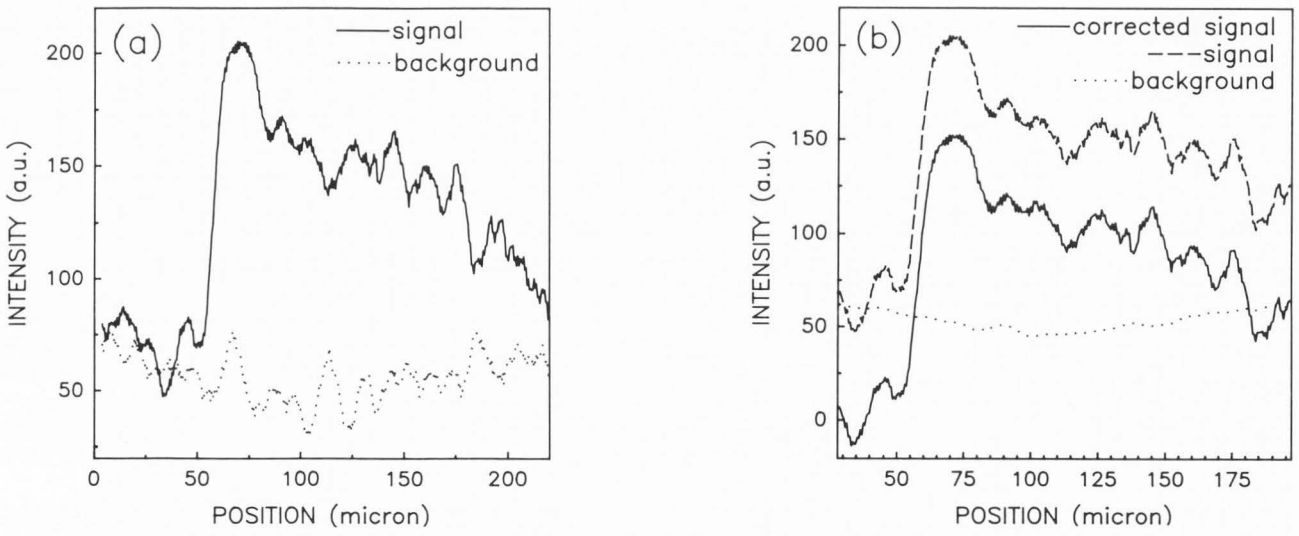

Figure 11. **(a)** 2 msec signal and background lines; **(b)** background subtraction.

when neglecting surface recombination. It is a few orders of magnitude higher than the density of free carriers in any semiconductor.

Discussion

Our thickness measurement method assumes that the main factor which governs the measured CL intensity is the exponential absorption of the substrate luminescence by the single phase superconducting thin film. The basis of the assumption is that for an opaque superconductor the major contribution to luminescence results from the shortest decay length which is perpendicular to the substrate-superconductor interface, and is represented by the thickness value. Our assumption is supported by the correlation with the secondary electron image, i.e. the highest contribution to luminescence was for regions which seemed thinnest in the SE image.

However, in order to generalize the model and for more accurate thickness determination, additional details should be considered in the model. These include both the electron beam interaction with the solid, and the optical properties of the sample itself. We draw here some outlines for such a treatment.

Concerning the electron beam interaction, the backscattered electron coefficient depends on the tilt angle between the beam and the surface. The amount of penetrating electrons varies accordingly, and therefore the density of generated carriers (see eq. 3) and light production is

changed. Furthermore, the effect of the thin superconducting layer on the electron beam penetration into the substrate should be considered.

Concerning the optical point of view, the fraction of the transmitted light depends on the surface properties. The light which is generated in the substrate is reflected via two interfaces: the substrate-superconductor interface, and the superconductor-vacuum interface. For a perfectly smooth surface a specular reflectance and transmittance occur, which obey Snell and Fresnel formulas. The fraction of specular transmission obeys the expression[13]:

$$\left(1-\left(\frac{n_1-n_2}{n_1+n_2}\right)^2\right)\left(\frac{n_1-(n_1^2-n_2^2)^{1/2}}{2n_1}\right) \qquad (4)$$

for transmission of light from material of a higher to a lower refraction constant., i.e for $n_1 > n_2$. For typical substrates such as MgO and $SrTiO_3$ the average values for the refraction indices are[9] 1.74 and 2.49, correspondingly. An estimate for YBaCuO could be derived from measured[8] values of the imaginary and real part of the dielectric constant, which gives $n \simeq 1.9$ for $YBa_2Cu_3O_{6.85}$. The fractions of transmission according to eq. 4 are 6.8% and 17.4% for YBaCuO-vacuum and $SrTiO_3$-YBaCuO interfaces, respectively.

The absorption as well as the multiple reflections in the substrate should be considered. The average absorption constants for the ordinary substrates such as MgO is[12] $8.1 \cdot 10^{-3}cm^{-1}$. For comparison, for the YBaCuO superconductor we derive a value of about $1.5 \cdot 10^{5}cm^{-1}$ according to the measured[8] values of the dielectric constant.

A rough surface causes the reflection to have a diffuse component, which does not obey eq. 4, and which causes a diffuse transmission and further loss of light. The ratio between the specular and diffuse reflection varies as a function of the surface roughness and of the wavelength. The surface roughness itself could be derived from the SE picture which is sensitive to morphology.

Conclusions

In the development of microscopic techniques for describing the high T_C superconducting samples, it was shown that different types of inhomogeneities can be examined by the CL method. It is a convenient nondestructive repetitive method. The information is obtained here at room temperature without the necessity to cool down the material to the superconducting transition temperature. Image processing of the CL pictures produces more quantitative information concerning both thin films and ceramic pellets.

Impurity phases embedded in a superconducting YBaCuO ceramic pellet were revealed through their strong cathodoluminescence. A detailed comparison of the luminescence signal for different microscope time scans was performed by the image processing method. The YBaCuO background was subtracted from the original signal for a more accurate profile. The lifetime of the impurity signal and the high density of the steady state carriers were thus estimated, which explained the intense luminescence signal. This method is applicable to any impurity phase having a long luminescence time. Impurity phases of different lifetimes would differ in their steady state carrier concentrations according to eq. 3. That could produce carrier gradients between nearby phases and could give rise to an electron beam induced current (EBIC[10]) signal.

We have shown for the first time the possibility to create thickness maps from the CL pictures, which correspond to single phase superconducting thin films free of substrate defects. The transformation to thickness map was done in real time, so that the SE, CL and thickness video images could be instantaneously compared. The gradual thickness variation within the sample was revealed through the histogram of the thickness image. The continuity of the film was shown at various threshold values, according to the fraction of the occupied area. At the conduction threshold value, the location and width of the weak links could be observed. Contour images provided mapping of only certain thickness values. This procedure may thus reflect the growth behavior of the film. For our working conditions, the lateral resolution was less than 1 μm, and the thickness resolution was of submicron and depended on the exact thickness value according to eq. 2. The work can be further extended to include the influence of the different optical properties of the superconducting film and the substrate on the resulting CL signal and thickness determination. This method may either be applied to a single phase film, as we have shown, or can be used for comparing samples of various thicknesses and morphologies. It may be applicable to any other high T_C superconducting film on an insulating substrate.

Acknowledgements

This research was supported by the Oren Family Chair for Experimental Solid State Physics, and the Israel Ministry of Science and Technology.

References

[1] Barkay Z, Azoulay J, Lereah Y, Dai U, Hess N, Racah D, Grunbaum E, Deutscher G. (1990). Cathodoluminescence study of thin films of high T_C superconductors. Appl. Phys. Lett. 57, 1808-1810.

[2] Barkay Z, Dwir B, Deutscher G, Grunbaum E. (1989). Electrical charging of percolating samples in the scanning electron microscope. Appl. Phys. Lett. 55, 2787-2789.

[3] Cooke DW, Jahan MS, Smith JL, Maez MA, Hults WL, Raistrick ID, Peterson DE, O'Rourke JA, Richardson SA, Doss JD, Gray ER, Rusnak B, Lawrence GP, Fortgang C. (1989). Detection of surface (~ 1 μm) impurity phases in high T_C superconductors. Appl. Phys. Lett. 54, 960-962.

[4] Cooke DW, Rempp H, Fish Z, Smith JL. (1987). Luminescent properties of X-irradiated rare-earth doped barium copper oxides. J. Mater. Res. 2, 871-875.

[5] Ehrenberg W, Gibbons DJ. (1981). Electron bombardment induced conductivity and its applications, Academic Press London, 66-67.

[6] Herrmann R, Reimer L. (1983). Backscattered coefficient of multicomponent specimens. Scanning, 6, 20-29.
[7] Huebener RP, Gross R. (1989). Simultaneous micro-characterization of the superconducting and structural properties of high T_C superconducting films. Scanning Microscopy 3, 703-710.
[8] Kelly MK, Chan Siu-Wai, Jenkin K, Aspnes DE, Barboux P, Tarascon JM. (1988). Optical characterization of surface and interface oxygen content in $YB_2Cu_3O_x$. Appl.Phys.Lett. 53, 2333-2335.
[9] Kingery WD, Bowen HK, Uhlmann DR. (1976). Introduction to ceramics, Wiley, New York, 646-677.
[10] Leamy HJ. (1982). Charge collection scanning electron microscopy. J. Appl. Phys. 53, R51-R80.
[11] Miller JH, Hunn JD, Holder SL, DiBianca AN, Bagnell CR. (1990). Use of cathodoluminescence microscopy to distinguish semiconducting from metallic phases in high T_C superconductors. Appl. Phys. Lett. 56, 89-91.
[12] Musikant S. (1985). Optical materials: An introduction to selection and application, Dekker, New York, 77-85.
[13] Reimer L. (1985). Scanning electron microscopy, Springer-Verlag, Berlin, 275-300.
[14] Yacobi BG, Holt DB. (1990). Cathodoluminescence microscopy of inorganic solids, Plenum Press, New York and London, 244.

Discussion with Reviewers

D.B. Holt: You identify weak links by thresholding. Have you tried checking that these are actually the sites of weak links e.g. by voltage contrast observations with the films biased and at room (or elevated) temperature?
Authors: We have not done 'voltage contrast' measurements of the weak links in the current work. But, we intend to perform such measurements on constricted geometries and to check the weak link behavior. Our previous experience in 'voltage contrast' corresponded to thin metallic percolating materials (see Z. Barkay et al., Thin solid films, 182, 97-104 (1989)).

D.B. Holt: Have you tried checking your thickness determinations using equation (2) by any other method?
Authors: The described film is one of a series of samples which was measured during preparation by a thickness monitor. The average thickness value was 2000Å.

G. Remond: Could spectral distribution changes resulting from either dielectric property changes of the specimen or beam damage, affect the total measured CL intensity and consequently affect the accuracy of the thickness determination?
Authors: The thickness method depends on the film absorption constant, and therefore should be applied to a single phase thin superconducting film (detected by x-ray diffraction for instance). An improvement of the method would be in producing monochromatic CL images at the substrate emission wavelength, in which case the detected luminescence would definitely originate from the substrate itself. Regarding our beam working conditions of V=30 keV and $I=10^{-9}$ A, the heating damage is insignificant. The temperature raise in the film can be estimated by $\delta T_{max} = 3P/2\pi x R_p$ (see ref. 13, p. 117). It yields 1.25 K, when the heating power (P=IV) is $3 \cdot 10^{-5}$ W, the thermal conduction is taken as $x \simeq 5 \cdot 10^{-6}$ W/μm K (Gross et al., IEEE Transactions on magnetics, 25, p.2250-2253 (1989)), and R_p = 2.3μm (see text). However, surface contamination could influence the precision of the thickness results. A clean environment, replacement of the diffusion pump by a turbomolecular pump, the use of minimum beam current and maximum voltage may all improve the precision of the results.

S. Myhajhenko: In the spectrally resolved ellipsometric work of Kelly et al., Appl.Phys.Lett.,53, p. 2333-2335, (1988), the dielectric properties as a function of wavelength of YBaCuO thin films in the spectral (detection) regime of your experiments (1.8-4.3 eV) were found to be strongly dependent on oxygen content. What are your comment on the possibility that variations in oxygen content may account for the CL contrast and apparent thickness variations in your measurements?
Authors: We prepared $Y_1Ba_2Cu_3O_{6+x}$ pellets of various oxygen contents $0.5<X<1$. We could not observe any difference in luminescence among the samples. There may be several reasons for that:(a) A too low beam current of 10^{-9}A which we ordinarily use. (b) Insufficient light collection, in which case a semiellipsoidal mirror could be added to improve the fiber optic collection of light. (c) The emission of YBaCuO due to lack of oxygen is at 4.1eV according to Kelly et al., which is actually the edge of our photomultiplier response. Whatever the exact reason for insensitivity to oxygen loss, we suppose that the cathodoluminescence information is not due to oxygen variations for $0.5<X<1$, but further experimental work should be done for the YBaCuO insulating range $0<X<0.5$.

S. Myhajhenko: A further comment on the panchromatic CL results concerns the origin of the luminescence. Since neither the substrates or thin films have been characterized from a spectroscopic perspective: the emission band from the substrate may not overlap the appropriate absorption regime of the thin films. In which case the origin and nature of the detected 'CL' contrast needs to re-evaluated. For example, the radiative decay of surface plasmons (enhanced by potential surface micro-roughness) in the thin superconducting films may well fall in the detected spectral regime of your experiments, see for example, 'Surface Plasmons' by H. Raether, Springer Tracts in Modern Physics Vol.III (1988). The spatial extent of these fields with depth goes as 1/e: this is similar to your assumption in Eq.1. Any comments on this possibility?
Authors: The emission band of the MgO substrate is at about 420nm. It was also confirmed in a more recent spectral CL measurement which we performed. Another common substrate as α-Al_2O_3 emits at 408nm (Hanusiak WM, White EW. (1975) Scanning Electron Microsc., I, p.125). For these emission wavelengths the absorption constant of YBaCuO is $1.5 \cdot 10^5 cm^{-1}$ (see the paragraph of discussion). Therefore the

substrate emission band may overlap the absorption regime of the thin film. As well, the intensity of light transmitted through the film surface is comparable to the intensity of a bare substrate, which means that their origin is probably similar.

S. Myhajhenko: You have estimated the generated steady state carrier concentration. This is indeed very high: what 'phase' of the matter would you expect the insulator to be in under these excitation conditions (e.g. electron-hole droplet,metallic, etc.?). Perhaps, the time constant of 0.7 ms you estimate is related to dielectric relaxation rather than excess carrier recombination. Any comments?
Authors: Dielectric relaxation occurred after electron beam charging of percolating 2D thin films (see ref. 2). The discharge of insulating grains appeared as flashes or streaks in the SE picture. Recently, we observed in the SE picture that thin superconducting films on insulating substrates can be charged and discharged as well in certain cases (unpublished yet). This electric relaxation primarily influenced the secondary electrons (SE picture) rather than the excess carriers (CL picture). But, in bulk superconductors we did not obtain SE variations for our SEM working conditions and typical scan times (0.02 to 128 sec per frame). This was probably due to the short discharging time constant associated with the low bulk resistivity. Therefore we claim that the typical time constant of 0.7 msec is due to excess carrier recombination rather than to dielectric relaxation.

B. Dwir: The authors state: "at 66%...conducting paths exist and the weak links can be recognized and located". When the CL signal is interpreted as thickness, it can show only relative values; it is arbitrarily assumed that maximum CL intensity corresponds to "zero" thickness (actually, it could be any base value). Unfortunately, the real (average) thickness of the films is not mentioned. Therefore, it cannot be assumed that the "connectivity threshold" in fig.6b corresponds to the thinnest point in the sample, or to a real electrical weak-link; there may still be considerable thickness below! Experimentally, it might be useful to measure the film thickness, or thickness profile (e.g. by micro-stylus profilometer, "alpha-step") and compare with the CL results.
Authors: The thickness values were obtained under assumption that the point of maximum CL intensity represented the substrate luminescence, and therefore corresponded to zero thickness. We could not measure luminescence from an uncovered region, as this sample and similar ones were completely covering the substrate. However, if the samples were prepared on part of the substrate, the film thickness could be determined without the need for this assumption. By 'weak links' we mean the ordinary physical interpretation of weak physical connected regions, such as grain boundaries and narrow or thin channels. By gradually varying the threshold thickness value, we could better distinguish slightly connected regions. These regions constitute weak link even if a lower thickness film surrounds them.

B. Dwir: The term "scaling", related to fig.10b, is unclear. Is it amplitude, distance or time scaling, and at what points were the two graphs normalized? I guess it is time scaling, and in this case the x-axis should be labeled accordingly. It seems that the time lags associated with the CL lifetime is better distinguishable in fig. 10a. Additionally, can the authors comment on a possible mechanism for the long lifetimes? could it be associated with charging effects of the insulating phases?
Authors: The CL profile was recorded as function of the beam position, in order to correlate the CL intensity with the point on the sample. The scanning beam velocity was constant, and therefore the total length is equal to the scan time up to a constant. The scaling refers to time scaling, because the 2 msec profile was divided by 4 to fit the 8 msec line profile. The two graphs converge at the left side of the luminescent grain boundary, which constitutes their origin. The scaled 2 msec CL graph and the 8 msec CL graph were therefore plotted as function of the beam position.
The long luminescence lifetime of 0.7 msec corresponds to phosphorescent materials (to distinguish from fluorescent materials of short lifetime). The mechanism responsible for the persistence of luminescence long after the excitation stops is the existence of trap levels besides the luminescent centers. The recombination time of the electron-hole at the luminescent center is governed by the Boltzman probability of escape of the carrier from the trap. Charging, if it exists, may influence the CL intensity, but the primary effect which governs here the grain luminescence is excess carrier recombination (see also answer to a similar question of S. Myhajhenko).

B. Dwir: The number of carriers should lead to quite a lot of emitted photons; can the authors give some estimate of the CL intensity compared with this number?
Authors: To estimate the number of emitted photons, it is necessary to consider the specular transmission factor, which is 6.8% for flat YBaCuO-vacuum interface (see discussion paragraph). Considering the rough grain surface (fig. 9c), the number of emitted photons is further reduced.